ELSEVIER

1 October 1998

PHYSICS LETTERS B

Physics Letters B 437 (1998) 35–43

Spin $\sim 60\ \hbar$ in ^{156}Dy: competition between collective and terminating structures at very high-spin

F.G. Kondev [a,1], M.A. Riley [a], R.V.F. Janssens [b], J. Simpson [c], A.V. Afanasjev [d,2], I. Ragnarsson [d], I. Ahmad [b], D.J. Blumenthal [b], T.B. Brown [a], M.P. Carpenter [b], P. Fallon [e], S.M. Fischer [b], G. Hackman [b], D.J. Hartley [a], C.A. Kalfas [f], T.L. Khoo [b], T. Lauritsen [b], W.C. Ma [g], D. Nisius [b], J.F. Sharpey-Schafer [h], P.G. Varmette [g]

[a] *Department of Physics, Florida State University, Tallahassee, FL 32306, USA*
[b] *Physics Division, Argonne National Laboratory, Argonne, IL 60439, USA*
[c] *CLRC, Daresbury Laboratory, Daresbury, Warrington, WA4 4AD, UK*
[d] *Department of Mathematical Physics, Lund Institute of Technology, S-22100 Lund, Sweden*
[e] *Nuclear Science Division, Lawrence Berkeley Laboratory, Berkeley, CA 94720, USA*
[f] *Institute of Nuclear Physics, NCSR Demokritos, 15310 Athens, Greece*
[g] *Department of Physics, Mississippi State University, Starkville, MS 39762, USA*
[h] *National Accelerator Centre, Faure, PO Box 72, ZA-7131, South Africa*

Received 14 April 1998; revised 14 July 1998
Editor: J.P. Schiffer

Abstract

The highest-spin discrete states ($I \sim 60\ \hbar$ and $E_x \sim 30$ MeV) in normal deformed nuclei have been observed in the rare-earth isotope ^{156}Dy using the ^{124}Sn(^{36}S,4n) reaction in conjunction with the GAMMASPHERE spectrometer. The positive parity yrast sequence appears to evolve smoothly from a prolate (collective) towards an oblate (non-collective) shape, in contrast to the sudden shape change observed in the isotone ^{158}Er. Terminating states are identified in the negative parity sequences at $I^{\pi} = 52^{-}$ and 53^{-} and specific multi-particle-hole configurations are assigned by comparison with cranked Nilsson-Strutinsky calculations. An order of magnitude increase in the interaction strength between close lying high-spin weakly collective structures is determined compared with that found in the lower-spin strongly collective domain. These results give valuable insight into the interplay between collective and terminating structures, and their competition for yrast status in the $40 - 60\ \hbar$ spin range.

PACS: 23.20.Lv.; 27.70.+q; 21.10.Re; 21.60.Ev
Keywords: High-spin collective structures; Band termination; Nilsson-Strutinsky cranking calculations; Bands interaction

[1] Corresponding author: Dr. F.G. Kondev, Tel.: +1 (850) 644 6226; fax: +1 (850) 644 9848; E-mail: kondev@nucott.physics.fsu.edu.
[2] Permanent address: Nuclear Research Center, Latvian Academy of Sciences, LV − 2169, Salaspils, Miera Str. 31, Latvia.

0370-2693/98/$ - see front matter
PII: S0370-2693(98)00938-1

The quest to observe increasingly high angular momentum states in atomic nuclei has helped drive the field of gamma-ray spectroscopy for many decades. Many surprising features have been discovered along the way and an ever blossoming variety of phenomena, exhibited by the nucleus as it builds up angular momentum, continues to be charted throughout the periodic table. It is in the transitional rare-earth region near $A \sim 150 - 160$ that the highest spin discrete states in both normal deformed ($I \geq 50\ \hbar$ [1,2]) and superdeformed ($I \geq 65\ \hbar$ [3]) nuclei have been discovered. It has been suggested [4,5] that it is precisely the co-existence of collective (prolate) and non-collective (oblate) structures at high angular momentum that creates a situation where a rapid funneling of the gamma-ray intensity down towards the yrast line occurs. Such a mechanism increases the probability of observing discrete, very high spin structures in normal deformed nuclei in this region.

Extensive experimental and theoretical studies have been carried out over recent years in the $N =$ 88-90 rare-earth nuclei. The accumulated results reveal that a prolate-to-oblate shape evolution occurs via the mechanism of band termination [6], which seems to be a general feature of these nuclei in the 35-50 $\hbar$ spin region. In fact, numerous examples are known, including ^{156}Er [7], ^{157}Er [8], ^{158}Er [9–11], ^{154}Dy [12,13], ^{155}Dy [14–17], ^{156}Dy [1,16,18], ^{158}Yb [19,20], ^{159}Yb [21] and ^{160}Yb [10,21]. A return to more collective behavior has also been observed in ^{154}Dy [13]. Furthermore, many more terminating structures are predicted (see for example Ref. [22] and references therein), but so far they have not been observed, either because their angular momenta are close to the maximum attainable from the accessible reactions or because their weak population precludes observation owing to limitations in the available detection systems.

In this letter we report the first observation of discrete levels with spin $I \sim 60\ \hbar$ in a normal deformed nucleus, ^{156}Dy, utilizing the high efficiency and resolving power of the Compton-suppressed Ge spectrometer array GAMMASPHERE [23], and discuss the competition between collective and terminating structures at very high spin.

States at high spin and excitation energy in ^{156}Dy were populated in the ^{124}Sn(^{36}S,4n) reaction using a 165 MeV beam from the 88″ Cyclotron at Lawrence Berkeley National Laboratory. The target consisted of two stacked 400 μg/cm^2 thick foils of ^{124}Sn. The GAMMASPHERE array comprised 93 large-volume Compton-suppressed Ge detectors. A total of approximately 1.3×10^9 events were collected, when five or more Ge detectors were in prompt coincidence. The data were unfolded off-line into $\sim 2.5 \times 10^{10}$ γ^3 coincidence events and incremented into a number of RADWARE [24] cubes. In order to enhance particular cascades in ^{156}Dy some of the cubes were selected in the sort with transitions in the band of interest.

The partial level scheme for ^{156}Dy, showing structures observed beyond spin 26 $\hbar$, is presented in Fig. 1. The levels are arranged in thirteen rotational sequences in accordance with the γ-ray coincidence relationships, and their ordering follows from the relative intensity of the transitions within a band. The assignment of spins was aided by the analysis of directional correlations from oriented states (DCO) [25]. Additionally, the identification of interconnecting transitions between sequences of the same parity and signature, (π, α), significantly strengthens the proposed assignments. While most of the bands are built upon previously known structures [1,18], the $(+,0)_3$, $(+,0)_4$, $(+,0)_5$, $(+,1)_1$ and $(-,1)_4$ bands are identified for the first time in the present work. (Note that although links between the $(+,0)_1$ and the $(+,0)_3$, and $(+,1)_1$ sequences have not been firmly established, the examination of individual coincidence spectra has shown that the latter two bands preferentially feed the $(+,0)_1$ band.)

Sample doubly-gated coincidence spectra showing the transitions depopulating the highest-spin states in the $(+,0)_2$, $(+,0)_1$ and $(-,1)_1$ bands are presented in Fig. 2. The current data confirm all gamma rays reported in the previous work of Morrison et al. [1], although some are placed differently in the level scheme, and extend most of the known sequences to higher spin. For example, the $(+,0)_2$ and $(+,0)_1$ bands have been extended from $I^\pi = 36^+$ and 46^+ to (62^+) and (58^+), respectively. These are *the highest spin discrete states* observed to date in a normal deformed nucleus and lie at excitation energies up to $\sim$ 30 MeV.

The $(-,0)_1$, $(-,1)_2$ and $(-,0)_2$ bands have been extended from 42^-, 41^- and 40^- up to 52^-, 49^-

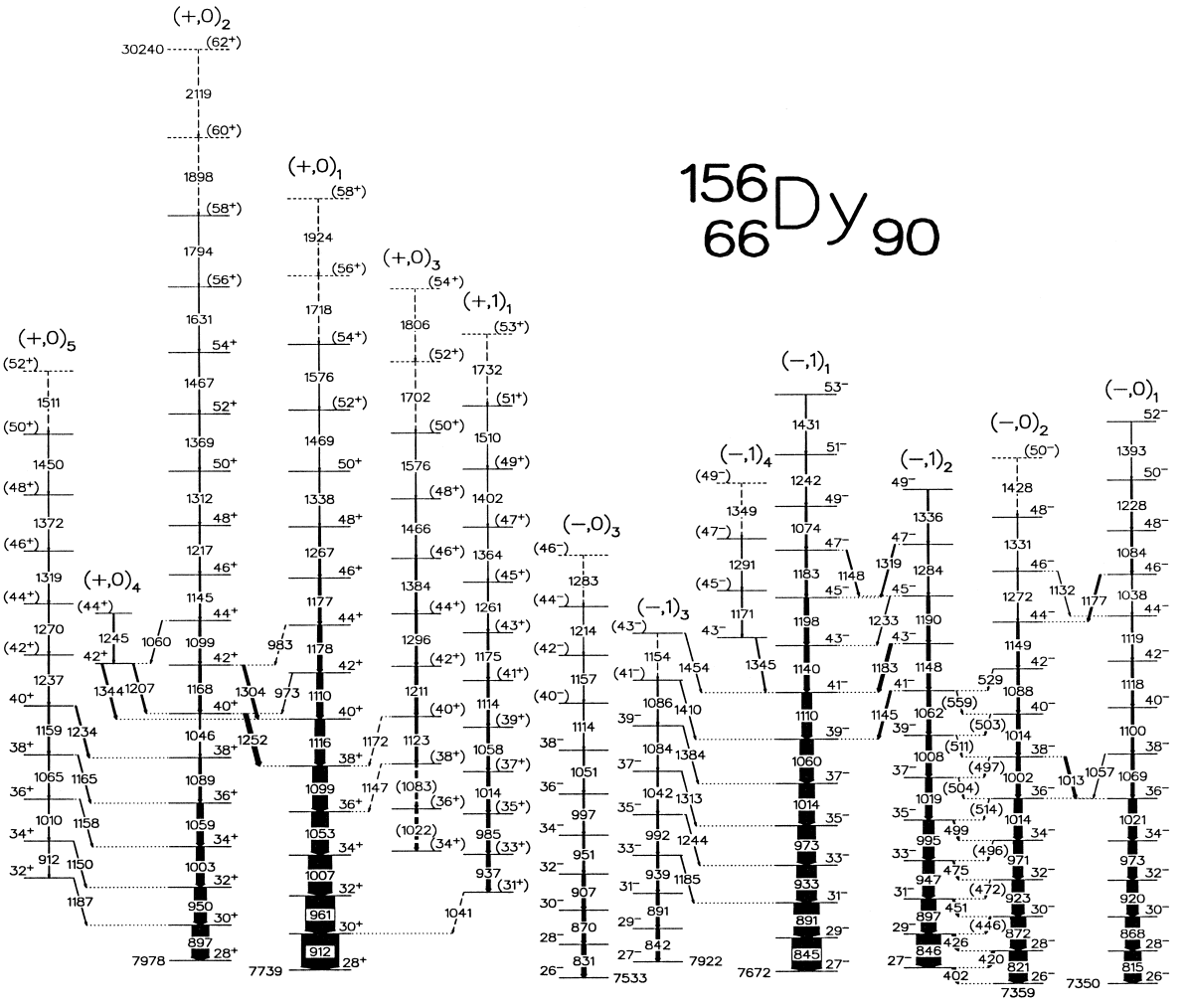

Fig. 1. Partial level scheme for ^{156}Dy showing states above spin 26 $\hbar$. The transition widths are proportional to the γ-ray intensities and the γ-ray energies are given to the nearest keV. Parentheses and broken lines indicate tentative assignments. The excitation energy of the lowest level shown in each sequence is indicated in keV along with that of the (62^+) state in the $(+,0)_2$ band.

and 48^- (tentatively 50^-), respectively. The $(-,1)_1$ band was not observed up to higher spin, presumably because this structure terminates at the 53^- state with no evidence for significantly intense transitions decaying to this state (see Figs. 1 and 2c). (A similar effect also appears to be present for the $(-,0)_1$ sequence at 52^-.) We assign the 1431 keV gamma ray as the $53^- \rightarrow 51^-$ transition, see Fig. 2c. This is in contradiction with Ref. [1], where a 1336 keV transition was suggested. In the current work the latter gamma ray is assigned to depopulate the 49^- state of the $(-,1)_2$ band, as shown in Fig. 1. The $(-,0)_2$ and $(-,1)_2$ bands experience a crossing with other sequences of the same parity and signature near 38^- and 39^-, respectively, which complicates the regular pattern. However, the identification of the 1013 keV gamma ray, the $38^- \ (-,0)_2 \rightarrow 36^- \ (-,0)_1$ inter-band transition, ties the ordering of the in-band transitions above 34^-. Importantly, it unambiguously places a 1002 keV gamma ray, the $38^- \rightarrow 36^- \ (-,0)_2$

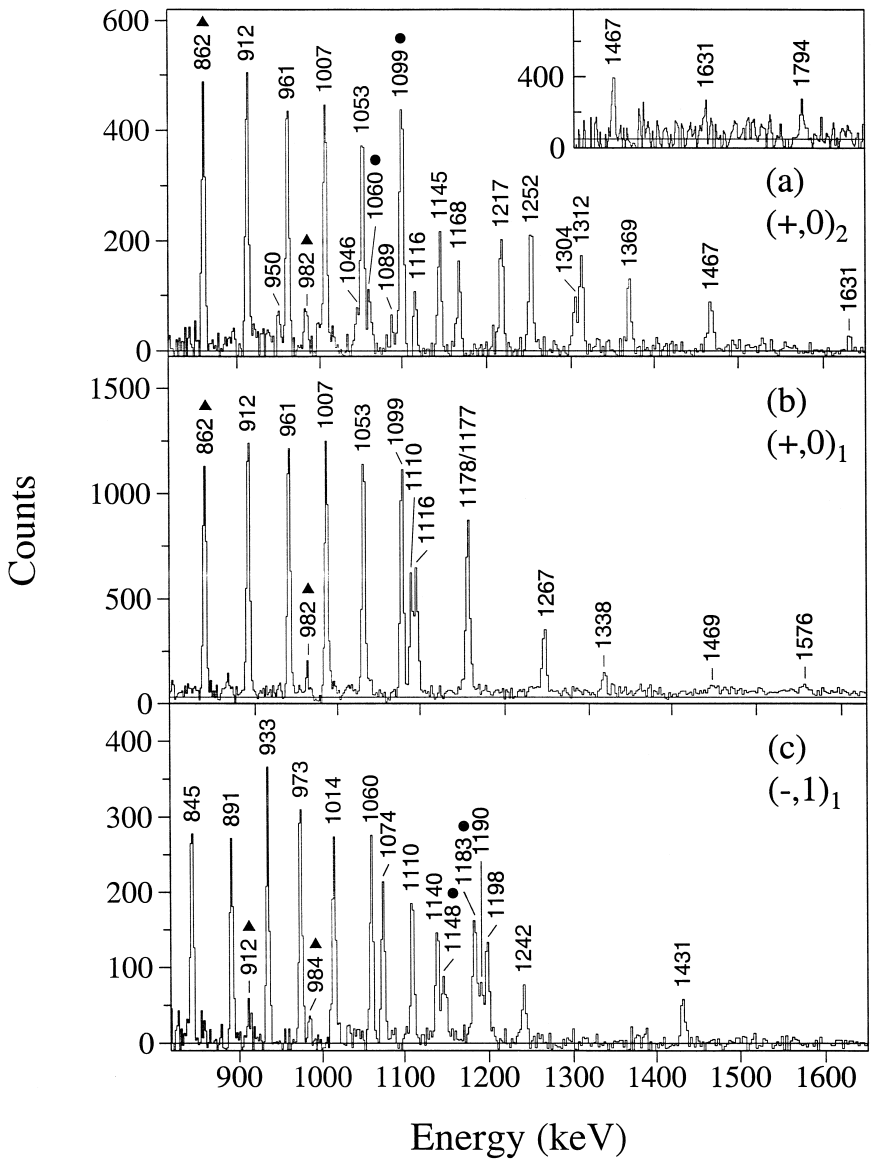

Fig. 2. Summed coincidence spectra. (a) Gates on all combinations of gamma rays de-exciting the 42^+, 46^+, 48^+, 50^+, 52^+ and 54^+, states in $(+,0)_2$ band. The inset shows a spectrum produced by summing gates on gamma rays de-exciting the 52^+ and 56^+ $(+,0)_2$ states with all transitions below 50^+ in the $(+,0)_2$ band and below 40^+ in the $(+,0)_1$ band. (b) Gates on all combinations of gamma rays de-exciting the 40^+, 42^+, 44^+, 46^+, 48^+, 50^+ and (52^+) states in $(+,0)_1$ band. (c) Gates on gamma rays de-exciting the 53^- and 51^- $(-,1)_1$ band levels with all gamma rays above the 17^- level of the $(-,1)_1$ band. The circles and triangles correspond to gamma rays which are doublets and those depopulating states with spins $\leq$ 28 $\hbar$, respectively.

in-band transition, between two gamma rays of similar energy, see Fig. 1. It is here that the current level scheme differs from that reported previously [1].

In order to interpret the behavior of the observed high spin structures in ^{156}Dy we have performed calculations based on the configuration-dependent, cranked Nilsson-Strutinsky formalism, described in detail in Refs. [22,26]. Within this approach different bands are formed by fixing a configuration, specified by the number of particles in different N-shells of

signature $\alpha = 1/2$ and $-1/2$, and searching, in a mesh of $(\epsilon_2, \epsilon_4, \gamma)$, for the lowest energy state at a given spin, thus treating the collective and non-collective states on the same footing. Potential energy surfaces as a function of spin were also obtained which allowed a distinction to be made between close-lying weakly-collective and fully-aligned structures within the same configuration. Additionally, the number of particles (holes) occupying orbitals of dominant high-j character, namely $h_{11/2}$ and $i_{13/2}$ for protons and neutrons is specified [28,29], but no distinction is made between the low-j shell orbitals, e.g. ($g_{7/2}$, $d_{5/2}$) and ($d_{3/2}$, $s_{1/2}$) for protons. The set of parameters given in Ref. [27], which is a standard in this region, has been employed with a small difference that a potential parameter $\mu = 0.6$ for the $N \geq 6$ proton orbitals has been used. Since pairing correlations are neglected in the present calculations, the results can be considered as realistic only at very high-spin, say above 35 $\hbar$. Figs. 3 and 4 present the results of our calculations in the form of excitation energy (minus a rigid rotor reference term) versus spin, together with the observations above $I = 25\ \hbar$. In general as discussed below, the calculations show a good overall correspondence with the experiment, albeit certain detailed questions remain and the predicted down-sloping (+,1) bands have not been observed (see Figs. 3c and 3d).

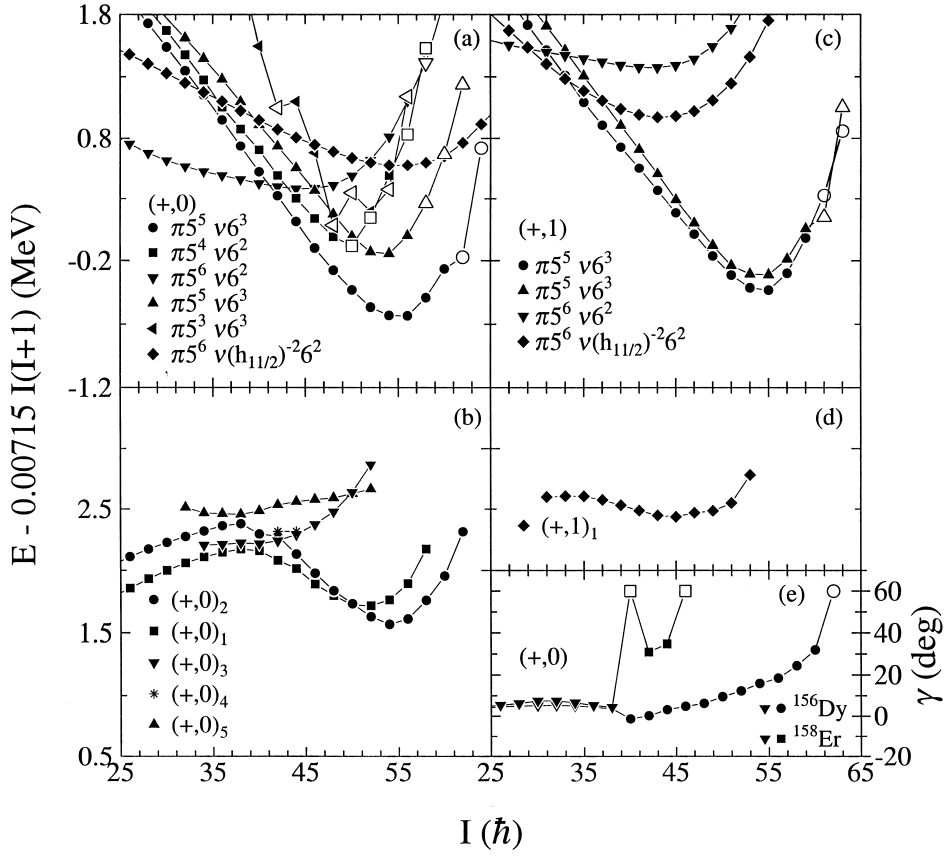

Fig. 3. Excitation energy minus rigid rotor reference, as a function of spin for selected positive parity bands. Theoretical predictions are shown in (a) (+,0) and (c) (+,1). The fully-aligned (oblate) states are indicated by large open symbols. Experimental values for the (+,0) and (+,1) bands are shown in (b) and (d), respectively. The contrasting changes in γ deformation as a function of spin for the calculated (+,0) yrast sequences in ^{156}Dy and ^{158}Er [11] are shown in (e).

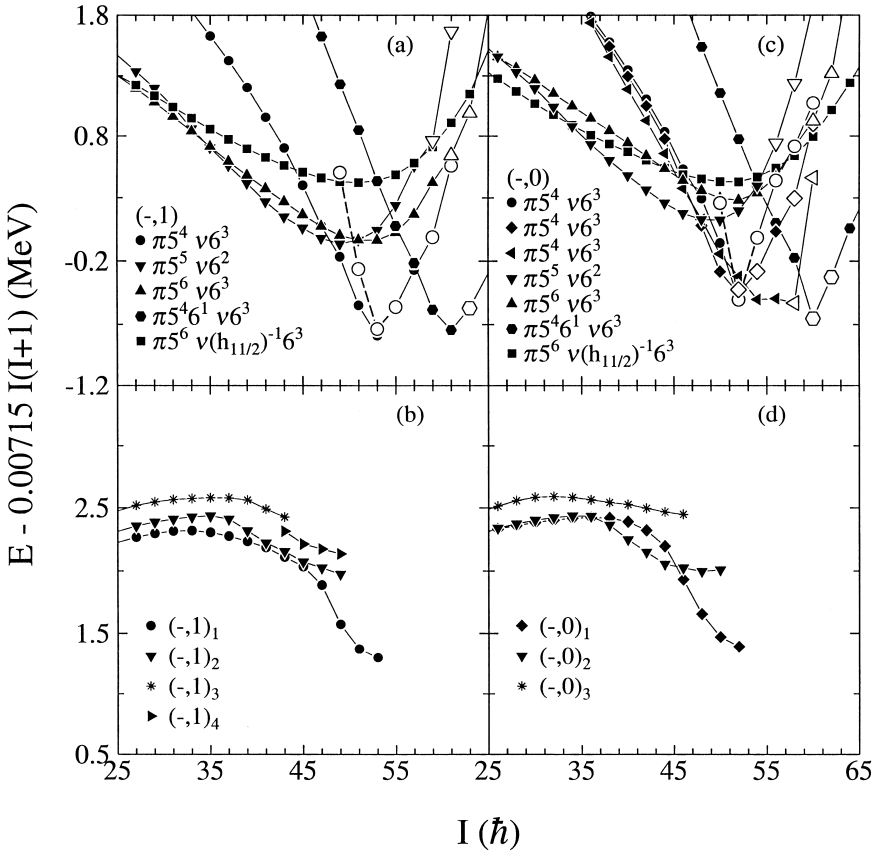

Fig. 4. The same as Fig. 3, but for negative parity bands. The dashed lines connect the states arising from the $\pi[(h_{11/2})^4,(d_{5/2}\,g_{7/2})^{-2}_{0^+X}]_{16^++X} \otimes \nu[(i_{13/2})^3,(h_{9/2}\,f_{7/2})^5]_{33^-}$ configuration, where $X = 0$, 2, 4 and 6 are for the $(-,1)$ sequences (a), and $X = 1$, 3 and 5 are for the $(-,0)$ sequences (c).

While the positive parity yrast band in the neighbouring isotone ^{158}Er shows features of *favored* band termination at 40^+ and 46^+ [11], since the last spin units are gained relatively cheaply in terms of energy, an unusual characteristic of the $(+,0)_1$ and $(+,0)_2$ bands in ^{156}Dy is the smooth bend upwards near 52^+ (band $(+,0)_1$) and 54^+ (band $(+,0)_2$). This behaviour means that close to the terminating point the angular momentum is obtained relatively expensively in terms of energy typical for an *unfavored* band termination as observed in the $A \sim 110$ mass region [28,29]. The comparison between theory and experiment suggests that the lowest energy $\pi 5^5 \nu 6^3$ $(+,0)$ configuration (the band shown with circles in Fig. 3a) can be assigned to the $(+,0)_2$ band. The deformation of this sequence evolves smoothly with increasing spin from $\varepsilon_2 \approx 0.19$, $\gamma \sim 0^o$ at 40^+ (prolate) through $\varepsilon_2 \approx 0.16$, $\gamma \sim 16^o$ at 54^+ (triaxial), and finally to $\varepsilon_2 = 0.10$, $\gamma = 60^o$ for 62^+ (oblate) with the aligned configuration $\pi[(h_{11/2})^5(g_{7/2}\,d_{5/2})^{-4}(d_{3/2})^1]_{29^-} \otimes \nu[(i_{13/2})^3 (h_{9/2}\,f_{7/2})^5]_{33^-}$. This can be traced in Fig. 3e where the predicted γ deformation as a function of spin for the $(+,0)$ yrast structure in ^{156}Dy is shown. For comparison, values obtained from calculations of the yrast structure of ^{158}Er [11] are also presented.

The highest spin part of the $(+,0)_1$ band is more difficult to interpret. The shape and minimum of the excitation energy minus rigid-rotor reference curve of the second $\pi 5^5 \nu 6^3$ configuration (up-triangles in Fig. 3a) fits reasonably well with the behavior of this band. However, this configuration is a ''double signature partner'' of the lowest $\pi 5^5 \nu 6^3$ configuration (circles in Fig. 3a) in the sense that the signatures of

the $N=4$ proton and $N=5$ neutron orbitals are reversed. Therefore, for this assignment, the crossing between the $(+,0)_1$ and $(+,0)_2$ bands at 50^+ is difficult to explain. The alternative $\pi 5^4\nu 6^2$ configuration (squares in Fig. 3a) seems to be unlikely as well because it terminates at 50^+ $(\pi[(h_{11/2})^4 (g_{7/2}d_{5/2})^{-2}]_{20^+} \otimes \nu[(i_{13/2})^2(h_{9/2}f_{7/2})^6]_{30^+})$. Although higher spin states can be formed within this configuration, for example by promoting protons from $(g_{7/2}d_{5/2})$ to $(d_{3/2}s_{1/2})$ orbitals across the $Z=64$ shell gap, as illustrated in Fig. 3a, this process is expected to be energetically unfavoured and would not lead to a ''smooth'' band.

For negative parity, Fig. 4, we associate the highest spin states of the $(-,1)$ band with the $\pi 5^4\nu 6^3$ sequence (filled circles in Fig. 4a) and the observed 53^- state with the $\pi[(h_{11/2})^4 (g_{7/2}\ d_{5/2})^{-2}_4]_{20^+}\otimes$ $\nu[(i_{13/2})^3\ (h_{9/2}f_{7/2})^5]_{33^-}$ multi-particle-hole configuration. This configuration is similar to that assigned to the 49^- state in ^{158}Er [11]. However, in ^{156}Dy the two proton holes contribute an additional 4 $\hbar$ units of angular momentum. Additional aligned states within the same configuration may occur when, for example, the proton holes couple to $I=0$, 2 and 6 $\hbar$ (these states are plotted with large open symbols and connected with a dashed line in Fig. 4a). The calculations predict that the first two configurations lie above the collective minimum at 49^- and 51^- (see Fig. 4a). In addition, the aligned 55^- state, formed from the maximal $(I=6\hbar)$ coupling of the two proton holes, is expected not to be as favoured as the 53^- state. These arguments may explain why these aligned states were not observed in the experiment. It should be noted, that the calculated $\pi 5^4\nu 6^3$ $(-,1)$ sequence has a weakly collective 53^- state which is almost degenerate with the fully-aligned 53^- state discussed above. Therefore, this band would terminate at either 53^- or 55^- depending on the energy splitting between the proton $g_{7/2}$ and $d_{5/2}$ orbitals. The experimental observation, however, suggest that the termination occurs at 53^-.

The calculations predict that three $\pi 5^4\nu 6^3$ $(-,0)$ sequences compete in energy above 44^-. The first favored terminating state is calculated to occur at 52^- with the configuration $\pi[(h_{11/2})^4$, $(d_{5/2}g_{7/2})^{-2}_3]_{19^+} \otimes \nu[(i_{13/2})^3,(h_{9/2}f_{7/2})^5_{16.5}]_{33^-}$. It is analogous to that already specified for the 53^- state, except that the two proton holes now couple to $I=3\hbar$. Alternatively, a fully-aligned 52^-, $\pi[(h_{11/2})^4, (d_{5/2}g_{7/2})^{-2}_4]_{20^+} \otimes \nu[(i_{13/2})^3$, $(h_{9/2}f_{7/2})^5_{15.5}]_{32^-}$ state can be assembled from the 53^- configuration by keeping the proton system unchanged, but promoting a neutron from $h_{9/2,\Omega=5/2}$ to $f_{7/2,\Omega=3/2}$. In fact, this configuration except for the two additional proton holes was assigned to the observed 48^- state in ^{158}Er [11]. The similarity in the energy differences between the 49^- and 48^- states in ^{158}Er ($\Delta E_x = 680$ keV [11]) and the 53^- and 52^- states in ^{156}Dy ($\Delta E_x = 670$ keV) supports the involvement of the latter configuration. Calculations predict that this aligned state is slightly above (~ 60 keV) a weakly collective level at 52^-, similarly to the situation at spin 53^- discussed above. Thus, the comparison between theory and experiment indicates that the energy splitting between orbitals arising from the $g_{7/2}$ and $d_{5/2}$ proton shells is underestimated in the present parameterization of the Nilsson potential.

The lowest two $(-,0)$ bands are observed to interact over a large range of angular momentum. Following the prescription outlined in Ref. [30] we have extracted the interaction strength from the experimental B(E2) ratios and the results are summarized in Table 1. Note that in cases where inter-band connecting transitions, depopulating both interacting levels are observed, the two deduced independent interaction strength values are consistent within the errors. In the region where the collectivity is sufficiently high (below $I\sim 40$ $\hbar$ [14]) the interaction strength between $(-,0)$ sequences is relatively small, i.e. less than 1 keV at 16^- and about 3, and 5 keV at 26^-, and 38^-, respectively. Since at low spin these band configurations are interpreted [18] as a coupling of the lowest $\nu i_{13/2}$ orbital with the $3/2^-[521]$ $(f_{7/2})$ or $11/2^-[505]$ $(h_{11/2})$ quasineutrons, respectively, and the latter two orbitals have opposite slopes in the Nilsson diagram, the interaction between them should be small [31]. Additionally, deformation differences between the two bands may also reduce the interaction, as detailed, for example in Ref. [32]. In this spin region the structures are expected to have stable prolate deformation with a preserved axial symmetry. Thus, a large difference in K quantum number $(\Delta K=4)$ between interacting bands may also be an important ingredient in quenching the interaction strength.

Table 1
Mixing matrix elements deduced from the B(E2) ratios

Band	I^π	E_γ (keV)		$\frac{B^{in}(E2)}{B^{int}(E2)}$	$\lvert V \rvert$
	($\hbar$)	in-band	inter-band		(keV)
$(-,0)_1[(-,0)_2]$	16^-				$\leq 1^{a)}$
$(-,0)_1$	26^-	760	767	0.96(7)	3(1)
$(-,0)_2$	26^-	777	769	1.79(11)	3(1)
$(-,0)_1$	38^-	1069	1057	> 0.05	> 2
$(-,0)_2$	38^-	1002	1013	0.43(3)	5(1)
$(-,0)_1$	46^-	1038	1177	1.02(27)	39(2)
$(-,0)_2$	46^-	1272	1132	0.37(5)	34(3)
$(-,1)_1$	41^-	1100	(1026)	≤ 0.27	$\leq 11^{b)}$
$(-,1)_2$	41^-	1062	1145	0.34(7)	12(1)
$(-,1)_1$	43^-	1140	(1104)	≤ 0.34	$\leq 10^{b)}$
$(-,1)_2$	43^-	1148	1183	0.52(17)	12(1)
$(-,1)_1$	45^-	1198	(1155)	≤ 0.17	$\leq 8^{b)}$
$(-,1)_2$	45^-	1190	1233	0.23(5)	9(1)
$(-,1)_1$	47^-	1183	1148	0.64(14)	16(1)
$(-,1)_2$	47^-	1284	1319	2.10(60)	17(2)

[a]) An upper limit taken as the half of the energy separation between the two 16^- levels. [b]) An upper limit deduced using the experimentally observed detection limit. Note that the transitions shown in brackets have not been directly observed.

The $(-,0)_1$ and $(-,0)_2$ bands interact again at 46^-, but the interaction strength is an order of magnitude greater than that found in the collective domain (see Table 1). Similarly, a large interaction occurs between $(-,1)_1$ and $(-,1)_2$ bands above spin 41 $\hbar$. These observations support the conclusions drawn in Refs. [10,22] that a larger wavefunction overlap occurs between different sequences for spin values above ~ 40 $\hbar$. Also, in this down-sloping region (Figs. 3 and 4) the structures become more triaxial, and as a consequence, more mixing will occur. Thus the importance of the K-value differences, as a factor in quenching the interaction, may tend to be gradually lost with increasing excitation energy and angular momentum.

In summary, many competing structures have been observed in the transitional $N = 90$ ^{156}Dy nucleus beyond spin 50 $\hbar$ and approaching $I = 60$ $\hbar$, representing the most comprehensive spectroscopic high-spin study of a nucleus so far. Comparisons with cranked Nilsson-Strutinsky calculations indicate that the two lowest energy positive parity bands undergo a smooth prolate-to-oblate shape evolution in contrast to that observed in the neighboring ^{158}Er nucleus. An enhanced interaction strength between weakly collective structures at high spin is observed contrary to that found in the strongly collective low spin domain.

The authors wish to extend their thanks to the staff of the LBNL GAMMASPHERE facility and the crew of the 88″ Cyclotron for their assistance during the experiment. The software support of D.C. Radford and H.Q. Jin is greatly appreciated. Support for this work was provided by the U.S. Department of Energy under Contract No. W-31-109-ENG-38, the National Science Foundation, the State of Florida, the U.K. Engineering and Physical Science Research Council and the Swedish Natural Science Research Council. MAR and JS acknowledge the receipt of a NATO Collaborative Research Grant. AVA and IR acknowledge financial support from the Crafoord Foundation (Lund, Sweden) and the Royal Swedish Academy of Sciences.

References

[1] J.D. Morrison et al., Europhys. Lett. 6 (1988) 493.
[2] J. Simpson et al., J. Phys. G 13 (1987) L235.
[3] S. Filbotte et al., Nucl. Phys. A 584 (1995) 373.
[4] J.C. Lisle, in Proceedings of the 5th Nordic Meeting on Nuclear Physics, Jyväskylä, Finland, 12-16 March 1984, p. 45.
[5] J. Borggreen et al., Nucl. Phys. A 443 (1985) 120.
[6] T. Bengtsson, I. Ragnarsson, Phys. Scr. T 5 (1983) 165.
[7] F.S. Stephens et al., Phys. Rev. Lett. 54 (1985) 2584.
[8] S.J. Gale et al., J. Phys. G 21 (1995) 193.
[9] P.O. Tjøm et al., Phys. Rev. Lett. 55 (1985) 2405.
[10] M.A. Riley et al., Phys. Lett. B 177 (1986) 15.
[11] J. Simpson et al., Phys. Lett. B 327 (1994) 187.
[12] H.W. Cranmer-Gordon et al., Nucl. Phys. A 465 (1987) 506.
[13] W.C. Ma et al., Phys. Rev. Lett. 61 (1988) 46.
[14] H. Emling et al., Phys. Lett. B 217 (1989) 33.
[15] R. Vlastou et al., Nucl. Phys. A 580 (1994) 133.
[16] M.A. Riley et al., Proc. of the Conference on Physics from Large Gamma-ray Detector Arrays, 2-6 August 1994 Berkley, CA; LBL-35687 Vol. II (1994) 206.
[17] T.B. Brown et al., to be published.
[18] M.A. Riley et al., Nucl. Phys. A 486 (1988) 456.
[19] C. Baktash et al., Phys. Rev. Lett. 54 (1985) 978.
[20] S.B. Patel et al., Phys. Rev. Lett. 57 (1986) 62.
[21] T. Byrski et al., Nucl. Phys. A 474 (1987) 193.
[22] I. Ragnarsson et al., Phys. Scr. 34 (1986) 651.

[23] R. Janssens, F. Stephens, Nuclear Physics News 6 (1996) 9.
[24] D.C. Radford, Nucl. Instrum. Methods Phys. Res. A 361 (1995) 297.
[25] K.S. Krane et al., Nucl. Data Tables , A 11 (1971) 351.
[26] T. Bengtsson, I. Ragnarsson, Nucl. Phys. A 436 (1985) 14.
[27] T. Bengtsson, Nucl. Phys. A 512 (1990) 124.
[28] I. Ragnarsson et al., Phys. Rev. Lett. 74 (1995) 3935.
[29] A.V. Afanasjev, I. Ragnarsson, Nucl. Phys. A 591 (1995) 387.
[30] G.J. Lane et al., Nucl. Phys. A 589 (1995) 129.
[31] G.B. Hagemann et al., Nucl. Phys. A 618 (1997) 199.
[32] G.D. Dracoulis, B. Fabricius, Phys. Rev. C 41 (1990) 2933.